

Creep Behavior of Nonburning Ti-35V-15Cr-xC Alloys

F.S. Sun and E.J. Lavernia

(Submitted August 24, 2005)

A comparison is made between the creep behavior of the Ti-35V-15Cr and Ti-35V-15Cr-0.2C alloys at 500 to 580 °C within the stress range of 200 to 300 MPa. The creep resistance of Ti-35V-15Cr-0.2C is considerably improved by the incorporation of Ti₂C particulates into the Ti-35V-15Cr-0.2C matrix.

Keywords dislocations, mechanical properties (creep), titanium alloys, transmission electron microscopy

1. Introduction

There is an interest in developing nonburning titanium alloys for aerospace applications. In 1985, Pratt & Whitney accelerated the development of a unique titanium alloy that would not burn under the operating condition present in an aeroengine to meet increasing demands in their industry sector. From this investigation, a commercial alloy, Ti-35V-15Cr, designated as alloy C, was developed that has high burn resistance up to 600 °C (Ref 1-3). Recently, an alloy development program was undertaken jointly by the Interdisciplinary Research Centre (IRC) at the University of Birmingham and Rolls-Royce that aimed to identify a low-cost nonburning titanium alloy by introducing Al into the Ti-V-Cr system; hence, an alloy of Ti-25V-15Cr-2Al was developed (Ref 4-6). In addition to the burn-resistant properties, there is great interest in optimizing the mechanical properties, such as creep resistance, of nonburning titanium alloys by investigating alloying effects. The objective of this research was thus to provide information on the significance of creep strengthening in carbon-bearing, nonburning titanium alloys.

2. Experimental

The alloys studied in this investigation were Ti-35wt.%V-15wt.%Cr and Ti-35wt.%V-15wt.%Cr-0.2wt.%C. Ten kilogram ingots of each alloy were melted using a consumable-electrode-arc-remelting furnace with a combination of master alloys and pure elemental materials. The ingots were forged into rods at 1000 °C and subjected to a heat treatment of 950 °C air-cooled (AC) and 1 h/700 °C AC for 4 h. Samples with a gage length of 50 mm and a diameter of 5 mm were used for creep testing. The experiments were performed on a vertical load frame with a 20:1 lever-to-arm ratio in air at 500, 540, and

This paper was presented at the Beta Titanium Alloys of the 00's Symposium sponsored by the Titanium Committee of TMS, held during the 2005 TMS Annual Meeting & Exhibition, February 13-16, 2005 in San Francisco, CA.

F.S. Sun and E.J. Lavernia, Department of Chemical Engineering and Materials Science, University of California, Davis, CA 95616. Contact e-mail: lavernia@ucdavis.edu.

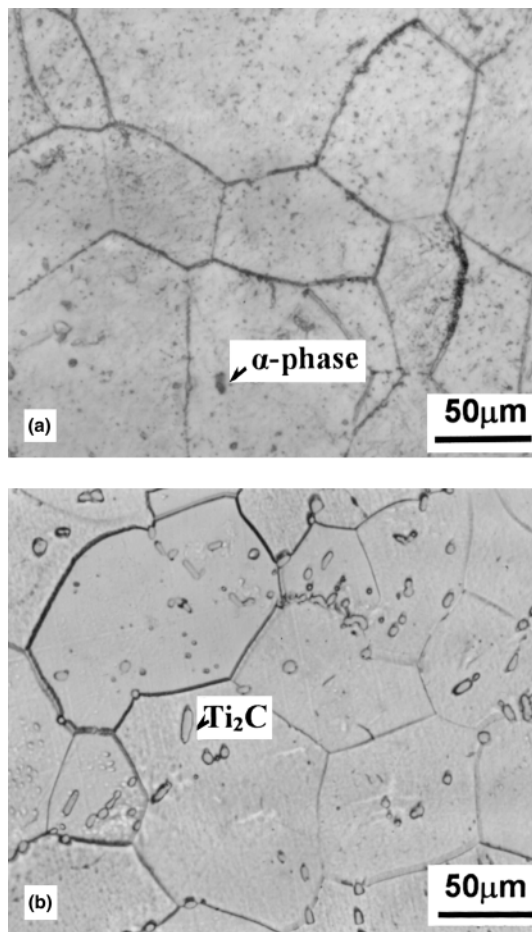


Fig. 1 Optical micrographs of (a) the Ti-35V-15Cr and (b) the Ti-35V-15Cr-0.2C alloys

580 °C, and 200 to 300 MPa. The testing temperature was measured using a thermocouple placed near the sample, and the variation of the temperature was within ± 5 °C. Creep deformation was recorded across the shoulders of the samples using a dial gage and a linear variable differential transducer. Engineering creep strain versus time curve was developed for each test, and the minimum creep rates were calculated from these curves. Microstructural characterization was conducted on the creep samples using an optical microscope. The deformation behavior was characterized using a transmission electron microscope (TEM).

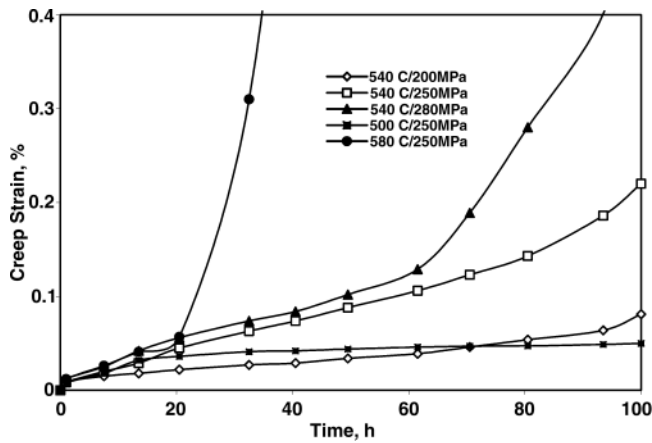


Fig. 2 Creep curves of the Ti-35V-15Cr alloy

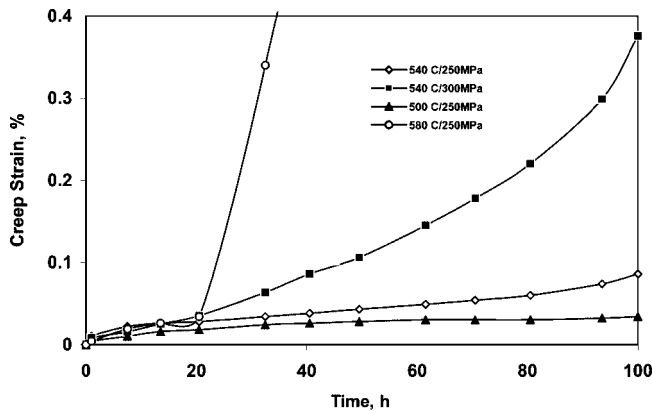


Fig. 3 Creep curves of the Ti-35V-15Cr-0.2C alloy

3. Results and Discussion

Optical micrographs of the heat-treated microstructures of the Ti-35V-15Cr and Ti-35V-15Cr-0.2C alloys are shown in Fig. 1. The microstructure of the Ti-35V-15Cr alloy consisted of a coarse β phase equiaxed structure with a grain size of approximately 108 μm , with some α phase in the matrix and the grain boundaries (Fig. 1a). The microstructure of the Ti-35V-15Cr-0.2C alloy consisted of a coarse β -phase matrix with Ti_2C particles randomly distributed in the matrix and the grain boundaries (Fig. 1b). The grain size was about 112 μm , and the average particulate size was determined to be 9.8 μm . Energy dispersive spectrometry (EDS) revealed that these Ti_2C particles consisted of 24.9 at.% C, 16.5 at.% O, and 58.6 at.% Ti.

Figures 2 and 3 show typical creep strain versus time curves for the Ti-35V-15Cr- $x\text{C}$ ($x = 0, 0.2\%$) alloys, which were obtained at temperatures of 500, 540, and 580 $^\circ\text{C}$, and applied stresses of 200, 250, and 280 MPa, demonstrating the three stages of the creep behavior: primary, secondary, and tertiary creep. It is clear that higher temperatures or higher stresses lead to a shorter secondary creep stage. The creep test results are presented in Table 1, which includes the creep deformation, the minimum creep rate, and the corresponding testing conditions for the heat-treated Ti-35V-15Cr- $x\text{C}$ ($x = 0, 0.2\%$) creep specimens. The data indicate that adding 0.2% C to the non-burning titanium alloys leads to greater creep resistance. For example, the creep deformation and minimum creep rate were

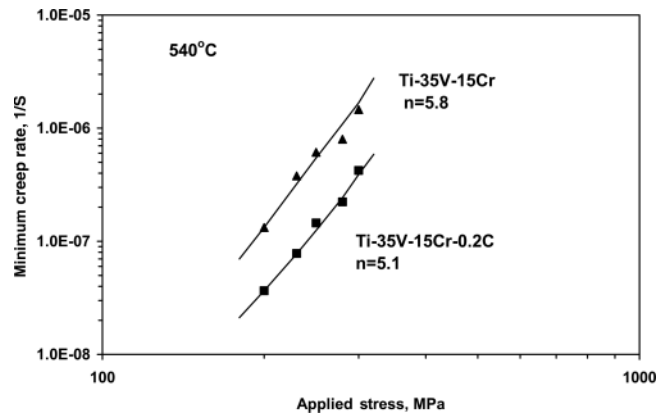


Fig. 4 Comparison of minimum creep rates of Ti-35V-15Cr- $x\text{C}$ ($x = 0, 0.2$) at 540 $^\circ\text{C}$

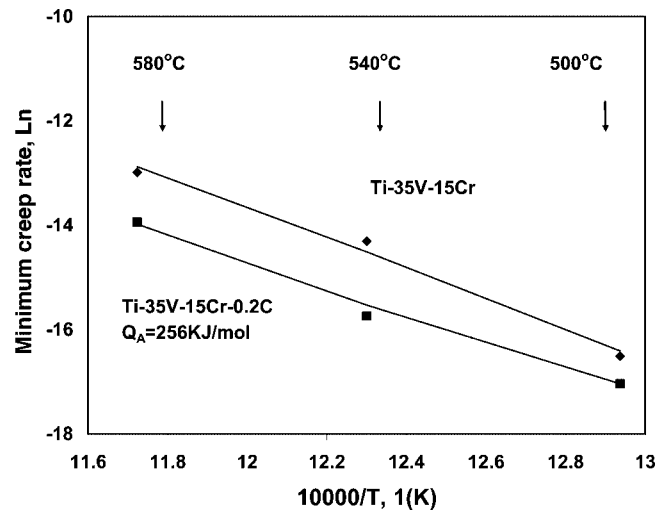


Fig. 5 Dependence of minimum creep rates on temperatures of Ti-35V-15Cr- $x\text{C}$ ($x = 0, 0.2$)

Table 1 Creep properties of the Ti-35V-15Cr- $x\text{C}$ alloys ($X = 0, 0.2\%$)

Alloy	σ , MPa/ Temperature, $^\circ\text{C}$	Creep deformation ϵ_p , %	Minimum creep rate ϵ_{\min} , 1/s
Ti-35V-15Cr	250/500	0.051	6.79×10^{-8}
	200/540	0.081	1.32×10^{-7}
	230/540	0.148	3.79×10^{-7}
	250/540	0.220	6.11×10^{-7}
	280/540	0.541	7.38×10^{-7}
	300/540	0.982	1.41×10^{-6}
Ti-35V-15Cr-0.2C	250/580	8.91	1.91×10^{-6}
	250/500	0.034	3.97×10^{-8}
	200/540	0.011	2.34×10^{-8}
	230/540	0.022	7.81×10^{-8}
	250/540	0.087	1.45×10^{-7}
	280/540	0.093	2.23×10^{-7}
	300/540	0.372	5.89×10^{-7}
	250/580	8.82	8.81×10^{-7}

more than three times greater for the Ti-35V-15Cr alloy than for the Ti-35V-15Cr-0.2C alloy at 540 $^\circ\text{C}$ /250 MPa.

The creep resistance is increased by incorporating Ti_2C par-

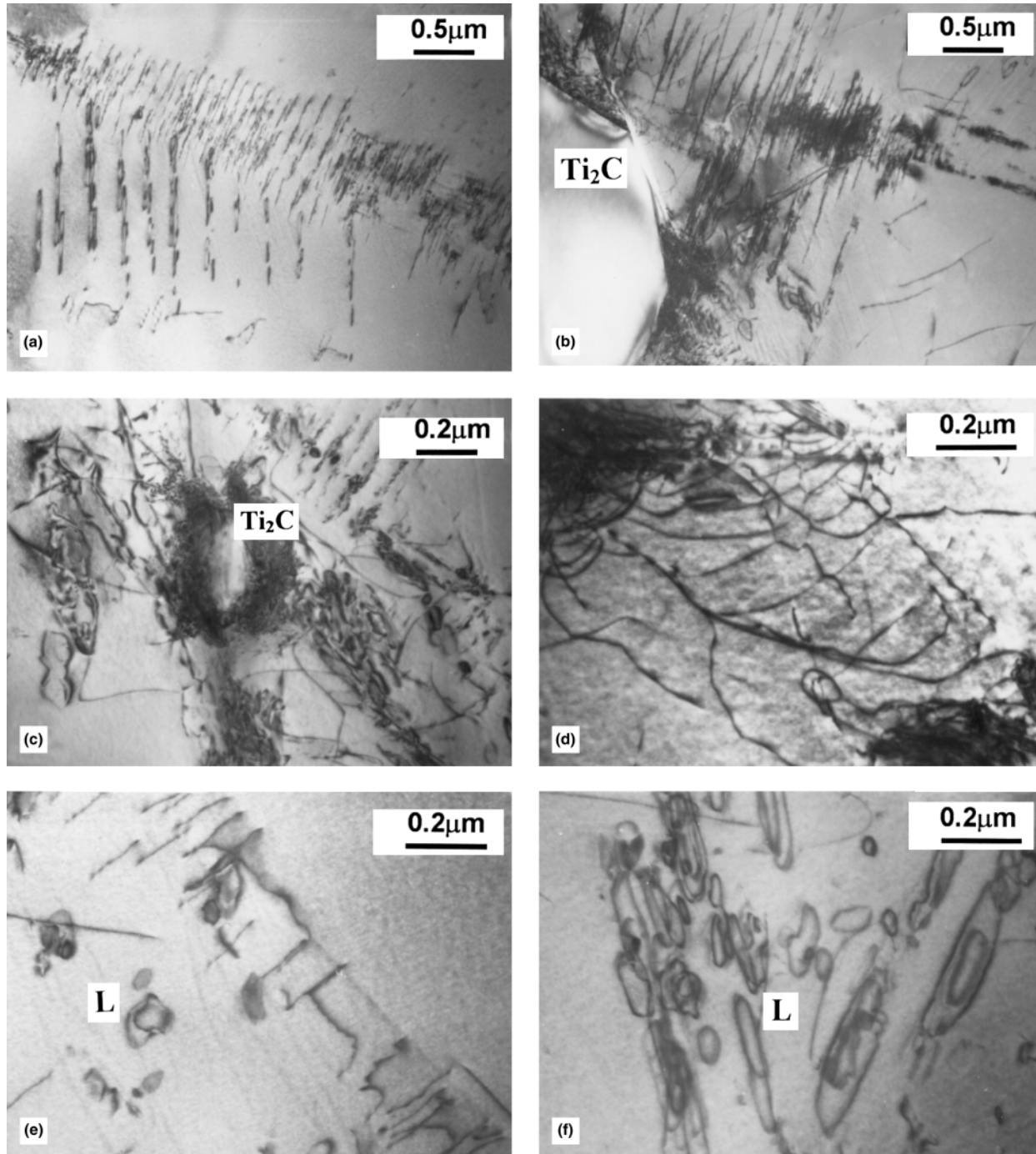


Fig. 6 Dislocation substructures observed in the Ti-35V-15Cr-0.2C alloy crept at 540 °C under 250 MPa

ticulates into the Ti-35V-15Cr-0.2C matrix and by solid-solution-strengthening of C in the matrix over the entire range of the applied stress from 200 to 300 MPa (Table 1). The creep parameters (n and Q_A) were calculated from the power-law creep equation from minimum creep rate:

$$\varepsilon_{\min} = A\sigma^n \exp(-Q_A/RT) \quad (\text{Eq 1})$$

where ε is the minimum creep rate, A is a constant, σ is the applied stress, n is the stress exponent, Q_A is the apparent activation energy for creep, R is the gas constant, and T is the absolute temperature. Figures 4 and 5 show plots of $\log \varepsilon_{\min}$ versus $\log \sigma$ at $T = 540$ °C and $\ln \varepsilon_{\min}$ versus $(1/T)$ at $\sigma = 250$

MPa, respectively, for the heat-treated Ti-35V-15Cr- x C ($X = 0, 0.2\%$) alloys. The strain-rate dependence on temperature exhibited classic creep behavior, where the slope, taken from the linear relationship between $\ln \varepsilon_{\min}$ and $(1/T)$, yields Q_A . The Q_A values obtained for Ti-35V-15Cr and Ti-35V-15Cr-0.2C are 291 and 256 kJ/mol, respectively, for an applied stress of 250 MPa (Fig. 5). As shown in Fig. 4, the creep exponents of 5.8 and 5.1, respectively, for the Ti-35V-15Cr and Ti-35V-15Cr-0.2C alloys were obtained for the stress range of 200 to 300 MPa. These creep exponents were constant, which suggests that a single mechanism was operating over the entire range of the applied stress.

Figure 6(a) to (f) shows dislocation substructures of the

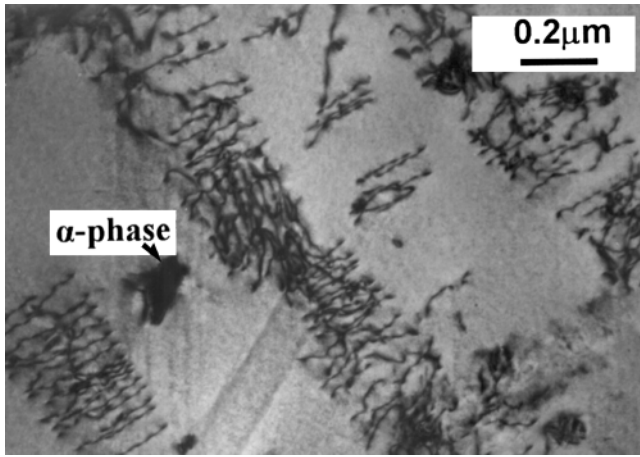


Fig. 7 Dislocation substructures observed in the Ti-35V-15Cr alloy crept at 540 °C under 250 MPa

Ti-35V-15Cr-0.2C alloy crept at 540 °C under 250 MPa pressure. The TEM investigations revealed that the slip of the dislocations was planar within β grains, while other straight dislocations were inclined to the slip plane, suggesting that secondary slip had occurred (Fig. 6a). Some dislocations occurred in pileup configurations at Ti_2C particle/ β phase boundaries, as shown in Fig. 6(b), suggesting that the large Ti_2C particles acted as obstacles to the motion of creep dislocations. The Ti-35V-15Cr-0.2C alloy (Fig. 6c) reveals prominent strengthening due to precipitated Ti_2C particles, showing dislocation pileup at the interfaces of Ti_2C precipitates. A different dislocation substructure was observed for the Ti-35V-15Cr-0.2C alloy (Fig. 6d), where bowed-out dislocations were moving on two slip systems. An unexpected but important aspect of the creep deformation structure in the Ti-35V-15Cr-0.2C alloy is the occurrence of loops in the β grains, as shown in Fig. 6(e) and (f), suggesting the presence of a dislocation climb/slip control mechanism for the creep deformation in the Ti-35V-15Cr-0.2C alloy. These loops may be directly related to dislocation climb and the result of vacancy or self-interstitial condensation. Different dislocation configurations were observed for Ti-35V-15Cr, which underwent creep at 540 °C with an applied load of 250 MPa, as shown in Fig. 7, with planar slip of dislocations and dislocation networks in the β matrix.

The presence of Ti_2C precipitates in the Ti-35V-15Cr-0.2C alloy remarkably improves the creep resistance, especially at 540 °C: the creep deformation and creep rate are reduced by a factor of three. The secondary creep behavior was characterized by stress exponent values greater than 5. It was therefore suggested that the creep deformation of the Ti-35V-15Cr- x C ($x = 0, 0.2\%$) alloys at 500 to 580 °C within an applied stress range of 200 to 300 MPa was dominated by a dislocation-controlled creep process, and this conclusion is supported by the observation of dislocation configurations. Dislocations and

loops were extensively observed in the matrix of the crept Ti-35V-15Cr-0.2C samples (Fig. 6a-f), indicating that the creep rate is controlled by a glide and/or climb mechanism. The secondary creep dislocation structure associated within this regimen indicated that dislocation pileup was occurring at the Ti_2C - β phase interfaces (Fig. 6b and c). If the glide and/or climb mechanism of the leading dislocations at the head of the pileup constitutes the rate-controlling mechanism, grain size and/or Ti_2C particle spacing with regard to the mean free-slip path would be important to the creep rate. The precipitation of Ti_2C particles in the Ti-35V-15Cr-0.2C alloy resulted in a decrease in the mean free-slip path, thus enhancing the creep resistance. This explains the lower creep deformation and minimum creep rates exhibited in the Ti-35V-15Cr-0.2C alloy compared with that of the Ti-35V-15Cr alloy. These results indicate that creep strengthening of the Ti-35V-15Cr-0.2C alloy occurs by second particle strengthening. The second particle-strengthening mechanism controls the creep behavior of the Ti-35V-15Cr-0.2C alloy when the matrix microstructure is constant and stable, and this alloy has good Ti_2C -matrix interface bonding (Fig. 6b), thus improving the creep resistance of the Ti-35V-15Cr-0.2C alloy.

4. Conclusions

The creep deformation and minimum creep rate of Ti-35V-15Cr-0.2C at 500 to 580 °C within the applied stress range of 200 to 300 MPa decreases significantly compared with that of Ti-35V-15Cr. The creep deformation of the Ti-35V-15Cr- x C ($x = 0, 0.2\%$) alloys was dominated by a dislocation-controlled creep process. The improved creep resistance of Ti-35V-15Cr-0.2C is attributed to second particle strengthening of Ti_2C particles by inhibiting the dislocation motion in the matrix.

Acknowledgment

The authors acknowledge the financial support provided by the Office of Naval Research (Grant No. N00014-04-1-0370).

References

1. D.M. Berczik, Age Hardening Beta Titanium Alloy, U.S. Patent 5176762, January 5, 1993
2. J.O. Hansen and D. Novotnak, Heat Treatment to Reduce Embrittlement of Titanium Alloys, U.S. Patent 5397404, March 14, 1995
3. P.A. Russo and S.R. Seagle, Enhancement of Hot Workability of Titanium Base Alloy by Use of Thermal Spray Coatings, U.S. Patent 5298095, March 14, 1994
4. Y.G. Li, P.A. Blenkinsop, M.H. Loretto, and N.A. Walker, Order-Disorder Transformation and Deformation Structure in β TiVCr Alloys, *Electron Microsc.*, Vol 2, 1998, p 59-60
5. Y.G. Li, P.A. Blenkinsop, M.H. Loretto, and N.A. Walker, Structure and Stability of Precipitates in 500 °C Exposed Ti-25V-15Cr-xAl Alloys, *Acta Mater.*, Vol 46, 1998, p 5777-5794
6. Y.G. Li, P.A. Blenkinsop, M.H. Loretto, and N.A. Walker, Effect of Aluminum on Ordering of Highly Stabilised β -Ti-V-Cr Alloys, *Mater. Sci. Technol.*, Vol 14, 1998, p 732-737